pressed index layers on the GVD is observed. However, the two notch layers are not quite as effective in producing negative dispersion as is the combination of asymmetry plus index notch. Since for physical realization the asymmetric structure is in fact more practical (e.g., cover layer being air), we can conclude that the four-layer asymmetric guide shown in Fig. 1(b) offers the best design possibilities. For example, a guide with the same parameters as curve $g = -16.6$ in Fig. 2, with $V = 3.22$ at $\lambda = 1.3\ \mu$m, will have $D = -55$ fs/nm · m (i.e., for a 100-nm bandwidth a 2-cm length guide has a total of −110 fs of negative guide dispersion).

Until this point, we confined ourselves to the TE modes. For TM modes, the determining equations are more complicated. However, it can be shown[4,5] that, for $\Delta n \ll n_i$, the universal normalized expressions for TE modes remain valid provided modified definitions are made for parameters a and g. These are

$$a_{\mathrm{TM}} = \frac{n_0^4}{n_{-1}^4}\frac{n_2^2 - n_{-1}^2}{n_0^2 - n_2^2}, \tag{11}$$

$$g_{\mathrm{TM}} = \frac{n_0^4}{n_1^4}\frac{n_1^2 - n_2^2}{n_0^2 - n_2^2}, \tag{12}$$

$$V_{1\mathrm{TM}} = \frac{n_1^2}{n_0^2} V_{1\mathrm{TM}}. \tag{13}$$

Thus, the curves shown in Figs. 2–4 can be used for TM modes as well but for the same values of n_0 and n_{-1} would correspond to different values of n_1 and n_2. For example, $n_0 = 2.4, n_{-1} = 1, n_1 = 2.07, n_2 = 2.37$ gives $g_{\mathrm{TM}} = -16.6$ and $a_{\mathrm{TM}} = 1060$. Due to the higher value of a, this TM case would give somewhat higher negative dispersion for a smaller value of notch depth than the $g = -16.6$, $a = 32$ TE case shown in Fig. 2. At the same time, it can be seen from Eqs. (12) and (13) that for the same d_1/d_0 value condition (9) remains unchanged. Thus the TM mode can be more effectively used to obtain negative GVD.

In conclusion, we have calculated the group velocity dispersion for both symmetric and asymmetric planar guides which are weakly guiding and have depressed index layer(s) next to the guiding region. We have found that the index notch is effective in producing negative guide dispersion. The various parameters make it relatively easy to adjust the dispersion. Thus, these guides may become useful in the future for integrated optics manipulation of ultrashort pulses.

References

1. R. L. Fork, C. H. Brito-Cruz, P. C. Becker, and C. V. Shank, "Compression of Optical Pulses to Six Femtoseconds by Using Cubic Phase Compensation," Opt. Lett. **12,** 483–486 (1987).
2. J. E. Bowers, P. A. Morton, and S. W. Sorzine, "Activity Mode-Locked Semiconductor Lasers," IEEE J. Quantum Electron. **QE-25,** 1426–1433 (1989).
3. A. Dienes, Y. Peng, and A. Knoesen, "Group Velocity Dispersion in Asymmetric Slab Guides," Appl. Opt. **28,** 12–14 (1989).
4. H. Kogelnik and V. Ramaswamy, "Scaling Rules for Thin-Film Optical Waveguides," Appl. Opt. **13,** 1857–1862 (1974).
5. D. W. Hewak and J. W. Y. Lit, "Generalized Dispersion Properties of a Four-Layer Thin-Film Waveguide," Appl. Opt. **26,** 833–841 (1987).
6. S. Kawakami and S. Nishida, "Characteristics of Doubly-Clad Optical Fiber with a Low Index Inner Cladding," IEEE J. Quantum Electron. **QE-10,** 879–887 (1974).
7. Y. Ohtaka, S. Kawakami, and S. Nishida, "Transmission Characteristics of a Multilayer Dielectric Slab Optical Waveguide with Strongly Evanescent Wave Layers," Trans. IECE Japn. **57-C,** 187–191 (1974).
8. Y. Peng, "Group Velocity Dispersion in Multilayer Planar Optical Waveguides," M.Sc. Thesis, U. California, Davis (1990), unpublished.
9. M. J. Adams, *An Introduction to Optical Waveguides* (Wiley, New York, 1981).

Polarization rotation in optical fibers due to geometric path variance

Jun Ye, Qu Li, Shao-Qing Peng, and Ying-Li Chen

Shanghai Jiao Tong University, Department of Applied Physics, Shanghai 200030, China.

Received 14 April 1989.
0003-6935/90/121724-03$02.00/0.

The geometric rotation of polarization in single-mode optical fibers is investigated theoretically and experimentally. The measurement results are reported for polarization rotation due to geometric path variance of single-mode fibers with the input and output ends of fibers being nonparallel.

Linear polarized light propagating through a monomode optical fiber of negligible intrinsic linear and circular birefringence and stress-induced effects will also produce the rotation of polarization as the geometric path is changed.

This effect was first studied by Ross[1] and Varnham *et al.*[2] Their theories are based on geometry and the axiom of parallel transport of light. When the input and output ends of fibers are parallel, the rotation is

$$\phi = -\int_{\text{input end}}^{\text{output end}} \tau ds.$$

Here τ is the torsion of the curve. In a uniform helix, this leads to $\phi = 2\pi(1 - P/S)$, where P is the pitch and S is the total length of fiber. Chiao and Wu[3] pointed out another method which was derived from Berry's phase factor in the adiabatic limit of quantum mechanics. When a system takes an adiabatic transport around a closed path in parameter space, a nonintegral phase factor will result which must multiply the wave function of the system. As linear polarized light travels along a helically wound optical fiber, a closed path C will form in momentum or $\mathbf{K}$ space and Berry's phase $\nu(c) = -\sigma\Omega(c)$.[4] Here $\sigma = \pm 1$ is the helicity quantum number of the photon and $\Omega(c)$ is the solid angle subtended by curve C with respect to the origin $\mathbf{K} = 0$. The phase factor is just the rotation angle of polarization. For a single-turn uniform helix, we have $\nu(c) = -2\pi\sigma(1 - p/s)$.

Then, how about the nonparallel case? It is obvious that, when the two ends of fiber are not parallel, a closed curve will not exist in $\mathbf{K}$ space, as shown in Fig. 1.

In Haldane's article,[5] the treatment using differential geometry is purely classical. On the unit $\mathbf{K}$ sphere, the initial and final wave vectors $\mathbf{K}_0, \mathbf{K}_1$ are separated because of the nonparallel input and output ends. We found a great circle connecting the two vectors, as shown in Fig. 1. Then a closed curve appears in $\mathbf{K}$ space and it spans a solid angle which is equal to the rotation angle of polarization. This fact is natural because a path lying along the great circle is a plane curve which will not raise polarization rotation according to

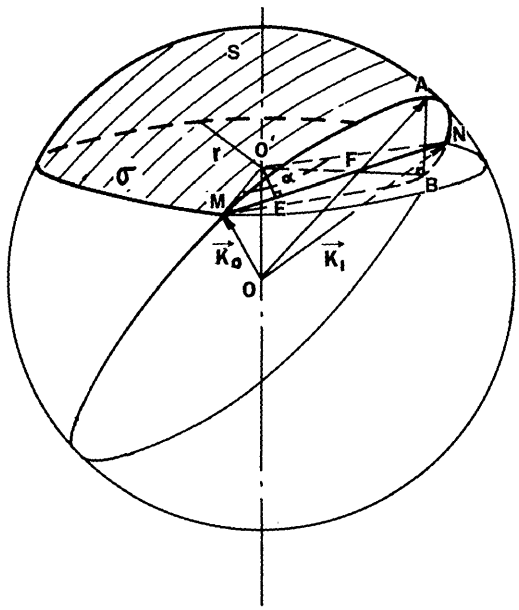

Fig. 1. Spherical surface in **K** space: $\mathbf{K}_0$, the **K** vector on the input end and $\mathbf{K}_1$, the **K** vector on the output end.

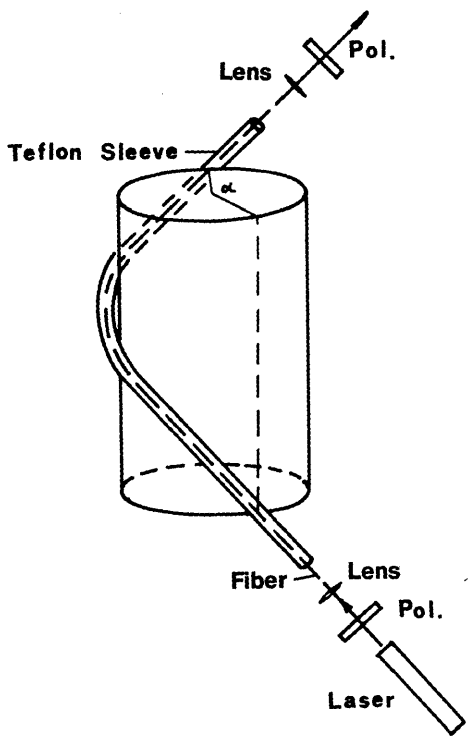

Fig. 2. Experimental setup.

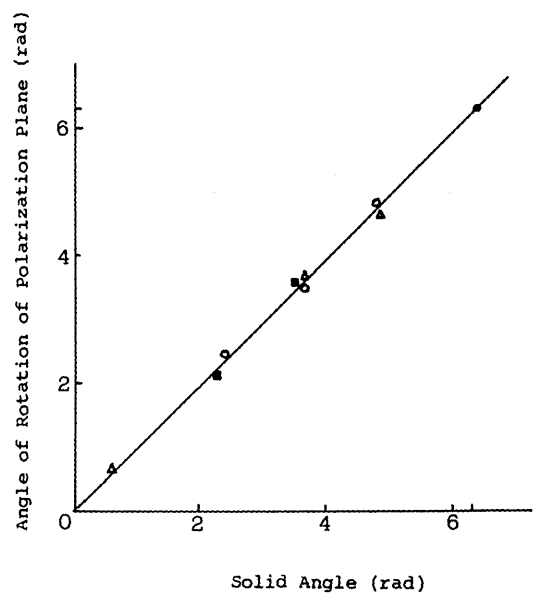

Fig. 3. Rotation angle of polarization with various fiber configurations: solid line, theoretical prediction; ●, measured for arbitrary plane curves; ○, measured for uniform helices; ■, measured for nonuniform helices; △, measured for the nonparallel case (a segment of uniform helices).

the parallel transport of light. So the rotation angle is just the shaded area shown in Fig. 1. The calculation of this area could be done as follows (see Fig. 1):

For any curved surface $Z = f(x,y)$, let us suppose $\partial f/\partial x = p$, $\partial f/\partial y = q$, and surface normal is $\hat{n}$. Then the surface area is

$$S = \iint_{(\sigma)} \frac{d\sigma}{\alpha s(\hat{n},\hat{z})} = \iint_{(\sigma)} \sqrt{1+p^2+q^2}\,dxdy$$

$$= \iint_{(\sigma)} \sqrt{1+p^2+q^2}\,rdrd\varphi.$$

In the unit sphere in **K** space, $|\mathbf{OM}| = |\mathbf{ON}| = |\mathbf{OA}| = 1$ and curve *MBN* is the projection of arc *MAN* in plane $\sigma \cdot O'E \perp MN$. Let the angle $\angle MO'N$ be written as α. Then

$$O'E = r \cdot \cos\left(\frac{\alpha}{2}\right),$$

$$O'F = O'E/\cos\left(\varphi - \frac{\alpha}{2}\right).$$

Here $\varphi = \angle MO'F$ is the angular coordinate measured from $O'M$.

Because $\tan(\angle OAB) = \tan(\angle O'OA) = O'F/OO'$, thus

$$\angle O'OA = \arctan(O'F/OO') = \arctan\left[\frac{r\cos\alpha/2}{\cos\left(\varphi - \frac{\alpha}{2}\right)\sqrt{1-r^2}}\right],$$

$$\begin{aligned} O'B &= O'F + FB \\ &= OF \cdot \sin(\angle O'OA) + AF \cdot \sin(\angle O'OA) \\ &= \sin(\angle O'OA). \end{aligned}$$

So the area of curved surface S is

$$\iint_{(\sigma)} \frac{R}{\sqrt{1-R^2}}\, dR d\varphi$$

$$= \int_{\alpha}^{2\pi} d\varphi' \int_0^r \frac{R}{\sqrt{1-R^2}}\, dR + \int_0^{\alpha} d\varphi \int_0^{O'B} \frac{RdR}{\sqrt{1-R^2}}$$

$$= (2\pi - \alpha)(1 - \sqrt{1-r^2}) + \int_0^{\alpha} d\varphi \int_0^{\sin(O'OA)} \frac{RdR}{\sqrt{1-R^2}},$$

where R is the radial coordinate.

The integration was worked out by computer. The experimental setup is quite simple, as shown in Fig. 2.

A 333-mm long monomode fiber was used in this experiment. It should be inserted loosely in a Teflon sleeve which was wound helically to reduce the torsional stress on the fiber during winding. Because the two ends of the fiber are nonparallel, the common transverse direction $(\mathbf{K}_0 \times \mathbf{K}_1)/|\mathbf{K}_0 \cdot \mathbf{K}_1|$ should be used to define the total rotation angle of polarization. A certain kind of refractive oil is smeared at the end of the input of the fiber to attenuate the cladding modes in fiber. The intrinsic birefringence (although very small), torsional stress, and the uncertainty of fiber path in the sleeve cause the dominant error in the experiment.

Table I. Polarization rotation for nonparallel case[a]

Parameters of helices	Radius / pitch	3.45 (cm) / 3.74 (cm)	1.55 (cm) / 19.73 (cm)	3.45 (cm) / 3.74 (cm)
α (deg)		33.0	14.0	112.0
Measured values (deg)		267.72	36.26	208.57
Theoretical prediction		4.742(rad) =271.69	0.623(rad) =35.72	3.609(rad) =206.77
Error (deg)		3.97	0.54	1.80

[a] See points Δ in Fig. 3.

Besides the nonparallel case, the uniform helix and nonuniform helix in which the two ends of fiber were kept identical were also studied. All data obtained in the experiment agreed very well with the theoretical value. The results are shown in Table I and Fig. 3. Here only the data of the nonparallel case are presented.

References

1. J. N. Ross, "The Rotation of the Polarization in Low Birefringence Monomode Optical Fibers Due to Geometric Effects," Opt. Quantum Electron. **16**, 455–461 (1984).
2. M. P. Varnham, R. D. Birch, and D. N. Payne, "Helical-Core Circularly-Birefringent Fibres," in *Technical Digest, Fifth International Conference on Integrated Optics and Optical Fiber Communication/Eleventh European Conference on Optical Communication*, Venice (1985), p. 135.
3. R. Y. Chiao and Y. S. Wu, "Manifestations of Berry's Topological Phase for the Photon," Phys. Rev. Lett. **57**, 933–936 (1986).
4. A. Tomita and R. Y. Chiao, "Observation of Berry's Topological Phase by Use of an Optical Fiber," Phys. Rev. Lett. **57**, 937–940 (1986).
5. F. D. M. Haldane, "Path Dependence of the Geometric Rotation of Polarization in Optical Fibers," Opt. Lett. **11**, 730–732 (1986).